Integrated transcriptomics and proteomics revealed the distinct toxicological effects of multi-metal contamination on oysters

Yunlong Li [a,b], Wen-Xiong Wang [b,c,*]

[a] Division of Life Science and Hong Kong Branch of the Southern Marine Science and Engineering Guangdong Laboratory (Guangzhou), The Hong Kong University of Science and Technology, Kowloon, Hong Kong, China
[b] School of Energy and Environment and State Key Laboratory of Marine Pollution, City University of Hong Kong, Kowloon, Hong Kong, China
[c] Research Centre for the Oceans and Human Health, City University of Hong Kong Shenzhen Research Institute, Shenzhen, 518057, China

ABSTRACT

The Pearl River Estuary (PRE) is the largest estuary in southern China and under high metal stress. In the present study, we employed an integrated method of transcriptomics and proteomics to investigate the ecotoxicological effects of trace metals on the Hong Kong oyster *Crassostrea hongkongensis*. Three oyster populations with distinct spatial distributions of metals were sampled, including the Control (Station QA, the lowest metal levels), the High Cd (Station JZ, the highest Cd), and the High Zn–Cu–Cr–Ni (Station LFS, with the highest levels of zinc, copper, chromium, and nickel). Dominant metals in oysters were differentiated by principal component analysis (PCA), and their gene and protein profiles were studied using RNA-seq and iTRAQ techniques. Of the 2250 proteins identified at both protein and RNA levels, 70 proteins exhibited differential expressions in response to metal stress in oysters from the two contaminated stations. There were 8 proteins altered at both stations, with the potential effects on mitochondria and endoplasmic reticulum by Ag. The genotoxicity, including impaired DNA replication and transcription, was specifically observed in the High Cd oysters with the dominating influence of Cd. The structural components (cytoskeleton and chromosome-associated proteins) were impaired by the over-accumulated Cu, Zn, Cr, and Ni at Station LFS. However, enhanced tRNA biogenesis and exosome activity might help the oysters to alleviate the toxicities resulting from their exposure to these metals. Our study provided comprehensive information on the molecular changes in oysters at both protein and RNA levels in responding to multi-levels of trace metal stress.

1. Introduction

The Pearl River Delta has become one of the most active industrialized regions, with millions of inhabitants and the high annual ecnomic output (trillions of US dollars) (HKTDC, 2020). Increasing industrialization has resulted in their direct discharges into the aquatic environment. Such intensive industrial activities lead to a typically high level of trace metals and threaten the organisms there. Trace metals occur naturally, and many of them are the essential elements for living organisms, such as copper (Cu), zinc (Zn), and nickel (Ni). Furthermore, trace metals are non-degradable, persistent, and relatively abundant in the environments. In this regard, it is important to monitor the contamination levels of trace metals as well as to evaluate the effects on local organisms, especially in the estuarine environments with intensive anthropogenic activities.

Estuarine areas are highly dynamic environments and are influenced by numerous factors such as tidal action, rainfalls, freshwater discharge, industrial sewage disposal, reclamation, and shipping (Dong et al., 2004; Tang et al., 2009). Metals in such environments can vary substantially over various tidal, daily, or seasonal cycles (Tan et al., 2018). Therefore, measurements of trace metal concentrations in a single time point could not reflect the overall status of the estuary. As such, biomonitors or bioindicators are used to manifest pollution levels in the environment. Oysters are regarded as the ideal candidates for metal contamination due to the sessile habitat and the ability to hyper-accumulate trace metals (Luo et al., 2014; Wang et al., 2011; Weng and Wang, 2015; Yin and Wang, 2017; Yu et al., 2013). Traditionally, ecotoxicological effects of metals are evaluated by the responses of several selected general

biochemical and physiological biomarkers in organisms (e.g., glycogen, catalase, metallothionein, and heart rate) (Chan and Wang, 2019; Liu and Wang, 2016a, b). However, most of these biomarkers might not be sensitive or applicable, and novel molecular biomarkers in oysters are needed to indicate the metal contamination level and toxicity.

The emerging omic tools could obtain high-throughput results in terms of the target organisms, and are more sensitive and specific in studying the molecular changes in organisms (Vailati-Riboni et al., 2017). RNA-sequencing (RNA-seq, also named as transcriptome) allows the detection of whole expressional profile at the transcript level (thousands of genes). The application of RNA-seq provides an important understanding of the molecular responses to toxicants in oysters, which can help discover new and specific genes potentially used as novel biomarkers. For example, Meng et al. (2018) employed RNA-seq to investigate the cellular toxicity of Pb and identified the endoplasmic reticulum as a biomarker. Comparative transcriptomics of oysters also found that cytoskeleton disruption was an indicator of severe metal stress (Li et al., 2020). Moreover, the mass spectrometry proteomics could detect much more proteins (thousands of them) with bioinformatics than traditional biochemical methods, which greatly favors our understanding at the protein level. The isobaric tags for relative and absolute quantification (iTRAQ) could further compare the corresponding expressions from different samples accurately (Wiese et al., 2007; Zhang et al., 2015).

However, poor correlation between mRNA and protein expressions was previously documented in a few earlier studies (Haider and Pal, 2013; Higdon et al., 2017; Peng et al., 2018). The possible reasons could be attributed to the post-translational modification (Parkes and Niranjan, 2019), inefficient translation (Taylor et al., 2013), resident time of protein and mRNA (Carneiro et al., 2019; Zhang et al., 2007), alternative splicing (Blencowe, 2006), and microRNA (O'Brien et al., 2018). Furthermoer, the negative correlation (e.g., high transcripts but low protein level) was also found, probably due to the transportation of

proteins among cells and tissues (Moritz et al., 2019). Therefore, it is important to validate whether these genes were also expressed differentially at the protein level. Integrated analysis of RNA-seq and proteomics thus provides a powerful approach since it can gain a more comprehensive insight at both mRNA and protein levels that might not be observed from a separated technique (Guerette et al., 2013; Kumar et al., 2016).

Well-controlled laboratory experimentation may depict the responses of organisms under established conditions but cannot reflect the actual status under the field conditions. Therefore, field study is necessary during the identification of biomarkers for environmental pollution. In the present study, three populations of oyster *C. hongkongensis* were sampled in the PRE. The oysters are native in the PRE and widely distributed in the inter-tidal area, including the east and west sides (Lam and Morton, 2003; Li et al., 2013). The transcriptomic and mass spectrometry-based proteomic analyses were integrated to construct the comprehensive database for the oysters under metal stresses at the RNA and protein levels. We hypothesized that the spatial differences of trace metals in PRE would differentiate the accumulated levels of trace metals and change the molecular profiles of oysters. Our study provided an understanding of the effects of trace metals on the field-growing oysters, and important information on evaluating the ecotoxicological risks by integrating omic tools.

2. Materials and methods

2.1. Oyster sampling

In this study, PRE was selected to study the molecular changes of field-collected oyster *C. hongkongensis* under metal accumulation (Fig. 1). During the spring tide (tide height < 50 cm), three oyster populations were collected since these organisms were in water most of the time.. Two oyster populations inhabited the west side of PRE: Station
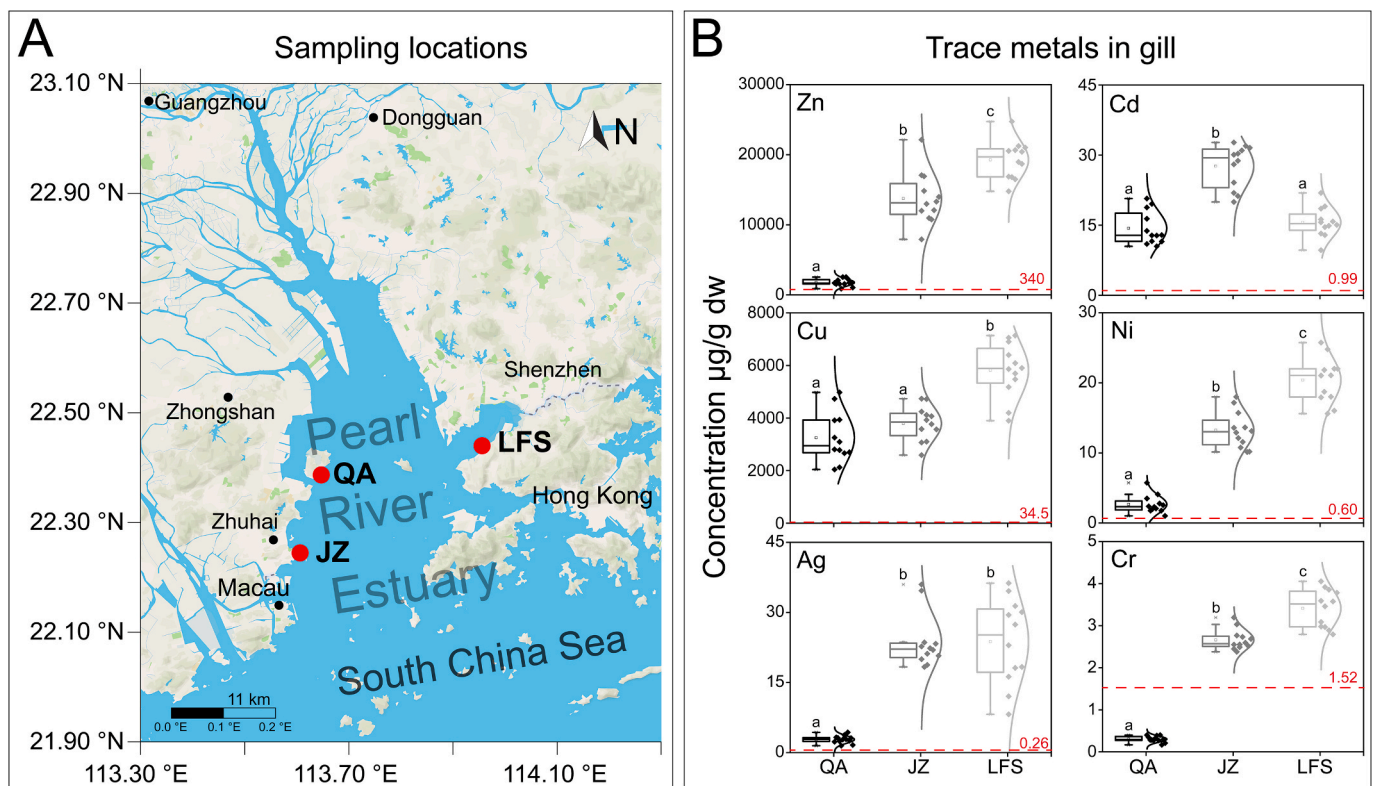

Fig. 1. A. Locations of three oyster populations in the Pearl River Estuary. QA: Qi'ao island in Zhuhai; JZ: Jiuzhou island in Zhuhai; LFS: Lau Fau Shan in Hong Kong. B. Concentrations of trace metals in the gills of oysters. Different letters signify the statistical difference between stations (*p* value < 0.001). The dashed line with red color indicates the baseline concentrations in oysters across China and the red figure indicates the specific amount (Lu et al., 2019).

QA (113.38 °E, 22.39 °N) in Qi'ao island of Zhuhai, and Station JZ (113.61 °E, 22.25 °N) in Jiuzhou island of Zhuhai. The other one was located on the eastern side, Station LFS (113.95 °E, 22.44 °N) in Lau Fau Shan, Hong Kong. There were 12 individuals with similar shell heights (about 8 cm) collected in each station. Previous studies documented that the physical factors (e.g., temperature, salinity, pH, and DO) would affect the expressional profiles of oysters (Dineshram et al., 2015; Li et al., 2019; Zhang et al., 2015; Zhao et al., 2012). Therefore, acclimation in the laboratory for two days was carried out before the dissection to avoid the possible effects on expressional profile from physical parameters among the three stations. The 2-d indoor acclimation would not lead to the significant decrease of metals in oyster *C. hongkongensis* due to the low elimination rates (Ke and Wang, 2001; Pan and Wang, 2009). These oysters were kept healthy, and there was no observed anomaly after the 2-d indoor acclimation at 24 ± 1 °C, pH 8.1, and salinity 15 ± 1 ppt (artificial seawater). The visible particles on the oyster surface were removed by ultra-pure water (Milli-Q, 18.2 MΩ, Millipore). For each individual oyster, the gill was divided into three pieces for metal determination, RNA-seq, and proteomics, respectively. All these samples were frozen by liquid nitrogen and stored at −80 °C until further experiments.

Before further analysis, polymerase chain reaction (PCR) was employed to check the species of oysters. In each population, 5 oysters were selected randomly for DNA extraction. Specifically, the genomic DNA of adductor muscle was isolated by Tissue DNA Kit (D3396-01, Omega Bio-Tek, USA), and then cytochrome oxidase subunit I (COI) fragment was amplified in ProFlex™ PCR (Thermo Fisher, USA) as described in previous studies (Li and Wang, 2021; Wang and Guo, 2008). As a result, all 15 samples owned the specific fragment (387 bp) of oyster *Crassostrea hongkongensis* (Fig. S1).

2.2. Metal determination

In total, 36 gill samples were freeze-dried (SCIENTZ, China) to remove moisture and used for metal concentration determination. About 100 mg samples were weighted for acid-digestion with 3 mL of 65% nitric acid (purris level, Sigma-Aldrich). The homogenized solution was obtained after 12 h of digestion at room temperature, followed by another 12 h at 80 °C. The levels of six metals (Cd, Cr, Cu, Ni, Ag, and Zn) were measured by inductively coupled plasma mass spectrometry (ICP-MS, NexION 300X, PerkinElmer). The efficiency of acid digestion was measured by the standard reference material (SRM 1566b, Sigma-Aldrich) via calculating the recovery of metals with the same procedure. During the analytical run, the multi-element standards (Quality Control Standard 21, PerkinElmer) were used as the quality control (QC) via monitoring the variation during ICP-MS detection, which was detected every 10 samples. In the present study, both the QC values and the recoveries of six metals (except for Cr without specified concentration in standard reference material) fluctuated from 90% to 110%.

2.3. Protein extraction and iTRAQ analysis

After frozen in liquid nitrogen, about 150 mg gill sample was milled into powder by a mortar and incubated in 1 mL lysis buffer (pH 8 Tris-base, 8 M Urea, 1% SDS, complete protease inhibitor cocktail) at 4 °C for 20 min. The supernatant containing total protein was obtained by centrifugation (12,000 g, at 4 °C for 15 min). The cold acetone with 10 mM DTT (4 vol) was mixed with the supernatant and then was kept at −20 °C overnight. The pellet collected by centrifugation was dissolved in 8 M Urea with Tris-base (pH = 8). Finally, 12 protein homogenates in each population were obtained (i.e., 36 ones in total).

Pooling strategy could be the alternative way to obtain the general expression of proteins, thus alleviating the difference among individuals (Kaur et al., 2012; Yan et al., 2014). In each population, 4 of 12 protein homogenates (from 12 replicated individuals) were randomly selected and mixed with an equal amount, resulting in 3 biological replicates.

Then, a 100 μg pooled sample was digested by trypsin Gold (Promega, USA), desalted by a Strata X C18 column (Phenomenex, USA), and then vacuum-dried. iTRAQ technique allows researchers to compare the relative abundance of proteins up to 8 samples in a single run simultaneously. In this study, the analysis of the total 9 samples was finished in 3 separated determinations with iTRAQ® Reagent-4PLEX Multiplex Kit (Applied Biosystems, USA). Specifically, 1 of 3 biological replicates in each population was labeled by isobaric tags (114 for Control, 115 for High Zn–Cu–Ni–Cr, and 117 for High Cd). Then, they were mixed for the following LC-MS/MS detection.

In each analytic run, the first 20 fractions of the sample were collected by the LC-20AB High-Performance Liquid Chromatography (HPLC) Pump system (Shimadzu, Japan). These fractions were firstly subjected to the EASY-nLC™ 1200 System (Thermo Fisher, USA) and then Q-Exactive HF-X mass spectrometer (Thermo Fisher, USA) for separation and mass determination, respectively. The threshold of mass acquisition was given below: positive polarity mode with capillary temperature of 320 °C for 1 h, full MS scan (range: 350–1500; resolution: 60,000; AGC target value: 3e6; Maximum IT: 20 ms), and data-dependent acquisition (fragment method: HCD spectra; TopN: 40; MS2 resolution: 15,000; Maximum IT: 45 ms; AGC target value: 1e5).

In the present study, the identification and quantification of proteins were slightly modified from our previous study (Li and Wang, 2021). The generated raw data (.raw) was firstly converted into mzML format via ProteoWizard (version 3.0.20192) and then subjected to Trans Proteomics Pipeline (TPP, version 5.2.0) (Deutsch et al., 2010; Kessner et al., 2008). The MS/MS search parameters in Comet (version 2017.01 rev. 0) were the suggested values by the developer, which is suitable for high res MS1 and high res MS2, and iTRAQ 4-plex (Eng et al., 2013). The database consisted of 29,482 proteins from the *Crassostrea hongkongensis* genome (Zhang et al., 2021) and their randomized peptides. The false discovery rate of predicted peptides was evaluated by the PeptideProphet (Nesvizhskii et al., 2003), and only peptides with false discovery rate (FDR) below 1% were subjected to iProphet for the protein prediction (Shteynberg et al., 2011). The threshold of reliable proteins was set as at least two unique peptides and FDR <1%. The Libra in TPP worked in quantifying the intensity of reporter ions (114, 115, and 117), which was used to compare the abundance of proteins among samples. The moderated *t*-test analysis was employed to compare the abundance of proteins, as Kammers et al. (2015) demonstrated. The criteria for differentially expressed proteins (DEPs) was fold-change < 0.87 or fold-change >1.15, with the moderate q value < 0.05. The principal component analysis (PCA) was conducted as mentioned earlier (Li et al., 2021). In the following sections, the fold-change of proteins in the bracket is shown for the result of proteomics unless otherwise noted.

2.4. RNA isolation and RNA sequencing

In each population, 5 gills from 5 individual oysters were selected to conduct RNA-seq. Total RNA of gill sample was extracted using TRIzol (Invitrogen, USA) under manufacture guidelines. The Agilent 2100 (Agilent Technologies, USA) was employed to check the RNA integrity number, and the Qubit® RNA Assay Kit with Qubit® 2.0 Fluorometer (Life Technologies, USA) was employed to measure the accurate RNA yield. Only high-quality RNAs (RIN >8.0 and RNA yield > 2 μg) were processed in the following steps. Briefly, mRNA with poly-A tail was enriched and then used for the cDNA synthesis and library construction by NEBNext® Ultra™ RNA Library Prep Kit (NEB, USA). In this study, more than 750 million short reads (150-bp Paired-End) were received by Hiseq 4000 (Illumina, USA) platform, which was deposited in the National Center for Biotechnology Information (NCBI), with the accession number PRJNA707394.

Trimmomatic was used to trim the adaptors and eliminate the low-quality reads (i.e., N content > 5% and the quality value of read < 20) (Bolger et al., 2014). Two scripts in Trinity (align_and_estimate_abundance.pl and abundance_estimates_to_matrix.pl) were employed

to evaluate the gene expression, including the valid reads of each gene (read counts) and Transcripts Per Million (TPM) (Bjärnmark et al., 2016). Of these, different tools were integrated, BOWTIE2 for reads mapping, and RNA-Seq by Expectation Maximization (RSEM) for quantification (Langmead and Salzberg, 2012; Li and Dewey, 2011). The R package DESeq2 comapred the gene expression among oyster populations to calculate the fold-change and the statistical level (Love et al., 2014). Blast (version 2.7.1) was employed to obtain the general annotation of those proteins and genes (Camacho et al., 2009). The Blast-KOALA helped to identify the pathway and ortholog of proteins (Kanehisa et al., 2016). In this study, differentially expressed genes (DEGs) were filtered by *q* value below 0.05, with the Station QA as the Control.

2.5. RT-qPCR verification

The real-time quantitative polymerase chain reaction (RT-qPCR) is an excellent method to study the relative abundance of genes at the mRNA levels. In total, the relative expressions of 11 genes in 15 samples (i.e., 5 replicated samples in each population) were checked by RT-qPCR, which was applied to check the reliability of RNA-seq and iTRAQ. The isolated RNA for RNA-seq was also suitable in this section. The RT-qPCR workflow details, including the primer design, reagents, and conditions, were described earlier (Li et al., 2021). The sequences of primers are shown in Table S1. Data acquisition was performed in LightCycler 480 II (Roche, USA). The amplification efficiency was assumed as 100% (i.e., ratio between the amplified sequence and the original template). Thus, the $2^{-\Delta\Delta Ct}$ method was adopted to calculate the relative expression, with the elongation factor 1α (EF-1α) as an internal standard.

2.6. Statistical analysis

Origin (version 2018) was employed to draw metal concentrations in the gill of oysters (i.e., and calculate the statistical difference (i.e., independent *t*-test). GraphPad (version 8.0) was used in calculating and visualizing the relationship among protein expression from iTRAQ, gene expression from RNA-seq, and RT-qPCR. The statistical significance of identified protein and differential analysis of expression was finished by the corresponding R package or software mentioned before. The threshold of significant differences varied in different calculations, shown in the above methods.

3. Results and discussion

3.1. Trace metals in different oyster populations

Based on the reports in the past ten years, the organic pollutants levels in PRE did not exceed the environmental criteria in China (Yu et al., 2021; Zhao et al., 2019). In details, PCB and DDT concentrations in sediments from our nearby collected sites were as low as 187.4 and 6.98 ng/g, respectively (Luo et al., 2014; Pintado-Herrera et al., 2017; Tang et al., 2020). Other organic contaminants such as polycyclic aromatic hydrocarbon (PAH) in the PRE was <1000 ng/g in sediments (HKEPD, 2020; Xiao et al., 2014) and <830 ng/L in water (Yu et al., 2021; Yuan et al., 2020), indicating that the threats by organic pollutants in PRE were not obvious. By comparison, trace metals were the major concerns in PRE, such as Cd, Zn, and Cu (Liu et al., 2017; Niu et al., 2020; Wang and Rainbow, 2020). Trace metals in estuarine waters varied greatly due to river discharge, whereas oysters could continuously accumulate trace metals, reflecting the history of metal contamination (Lu et al., 2020).

In this study, a native species, Hong Kong oyster *C. hongkongensis* was selected to monitor the spatial patterns of trace metals in the PRE. Gill plays a key role in accumulating and further responding to metals. Lu et al. (2019) conducted the cumulative frequency distribution analysis

of trace metals in oysters across China and proposed the 5% cumulative values as the baseline concentrations, which are indicated as the red values and dashed line in Fig. 1B. The concentrations of trace metals in the gill of oysters from PRE were much higher than the baselines (except for Cr at Station QA), implying severe metal contamination in the PRE (Fig. 1B).

Nonetheless, a clear spatial pattern was observed in this study. The top two PCA components (PC1: 71.4% and PC2: 18.6%, explaining 90% variance) distinguished them well and indicted the dominant metals (Fig. 2): Cd for Station JZ, Ag for both stations, the other four metals (Cu, Zn, Ni, Cr) for Station LFS. As shown in Fig. 1B, the lowest concentrations of all six trace metals were found in oysters from Station QA (1769 μg/g for Zn, 3250 μg/g for Cu, 2.81 μg/g for Ag, 14.25 μg/g for Cd, 2.66 μg/g for Ni, and 0.30 μg/g for Cr). In our study, the main objective was to study the effects of metals on oysters within PRE. The three stations were only separated by short distances, and the genetic backgrounds of oysters in this study were similar or the same (Fig. 1A). Therefore, it was feasible to consider Station QA as the control in the following RNA-seq and iTRAQ analysis, although the metal levels in oysters from this station were higher than the nationwide baseline values (except for Cr).

Except for Cu in Station JZ and Cd in Station LFS, oysters in these two stations contained statistically higher levels of the other metals than Station QA. Oysters at Station JZ accumulated the highest Cd, with 27.63 μg/g (1.9 times as that at Station QA) in the gill tissue. A similar Ag level was observed at both Station JZ and LFS, i.e., 23.7 μg/g (8.43 times as that of Station QA). The other four trace metals pointed to the Station LFS, which contained the highest levels of metals, i.e., up to 19,270 μg/g for Zn (10.9 times as that at Station QA), 5820 μg/g for Cu (1.78 times), 20.4 μg/g for Ni (7.8 times), and 3.41 μg/g for Cr (11.3 times). Therefore, the three stations were labeled according to their dominant metals, Control (Station QA, the lowest levels), High Cd (Station JZ, the highest Cd), and High Zn–Cu–Cr–Ni (Station LFS, with the highest levels of Zn, Cu, Cr, and Ni).

3.2. Integrated analysis by RNA-seq and iTRAQ

RNA-seq was applied to evaluate the expression of protein-coding genes. Among the 29,482 protein-coding genes, 18,185 (61.68%) were detected as expressed genes at the transcript level with the effective reads (count > 0), and their expressions were further compared in oysters from three stations. The transcriptional profiles of three oyster populations were distinguished from each other, with different levels of metal burden (Fig. S2A). Compared to Control (Station QA), a comparable number of DEGs was identified in the more contaminated oysters (944 at High Cd and 962 at High Zn–Cu–Ni–Cr) (Fig. 3B).

Generally, more than 1.2 million spectra were generated from the three analyses of LC-MS/MS. With the threshold of at least two unique peptides and FDR <0.01, LC-MS/MS analysis identified 3758 proteins in total from three analytic runs, 2949 in the first run, 2977 in the second run, and 3027 in the third run (Fig. S2B). Only proteins found in all three runs were quantified and were then proceeded in differential analysis of their abundance among populations, i.e., 2264 proteins in this study (Fig. S2B).

As mentioned before, the altered genes at the transcript level might not be consistent with the expression at the protein level. In this regard, integrating proteomic and transcriptomic approaches would overcome the shortcomings, screening out the corresponding proteins and genes under metal stress. In this study, we identified 2250 proteins, which became the database of the following in-depth investigation (Fig. 3A). All the abundance values of proteins (at both transcript and protein levels) are shown in Table S2. The principal component analysis of 2250 protein abundance implied the discriminated characteristics of proteins among three oyster populations, and the distribution of each population at protein abundance was similar to the trace metal concentrations in oysters, implying the role of metal contamination on the expressional profile (Fig. 3C). Thus, the protein-related method could be the better
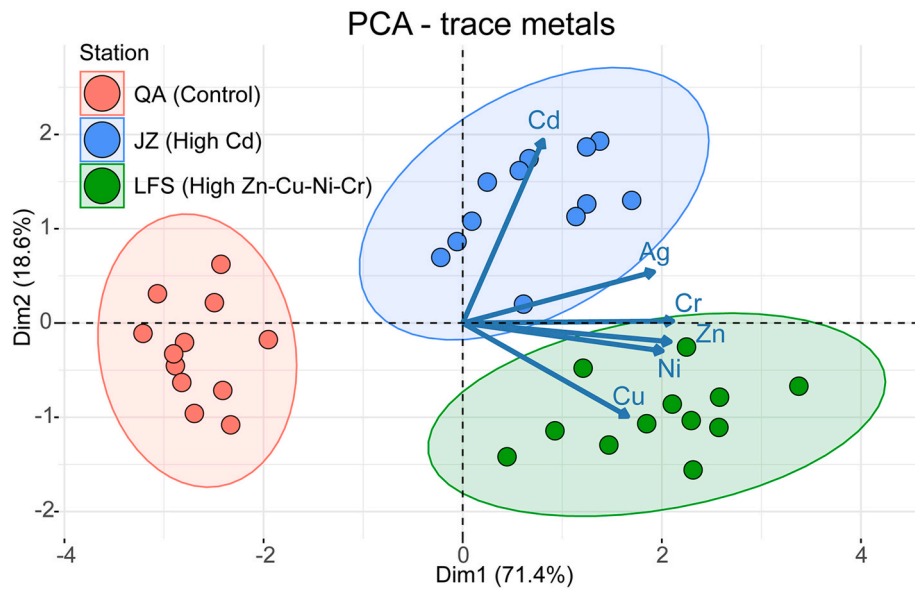
Fig. 2. The principal component analysis of traces metals in three oyster populations from PRE.
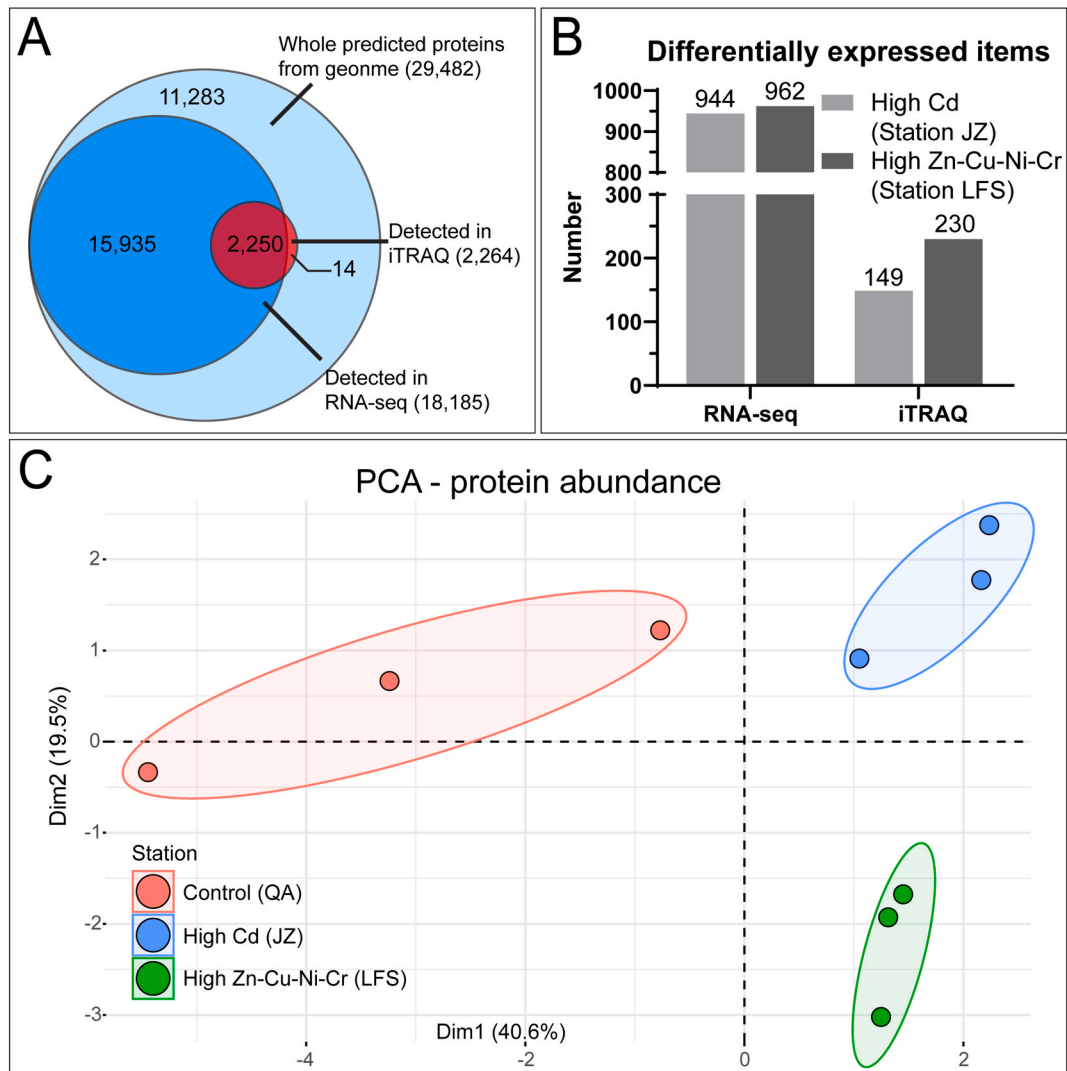

Fig. 3. (A) The number of identified proteins in three runs. (B) The number of proteins with differential expression at High Cd (Station JZ) and High Zn–Cu–Ni–Cr (Station LFS). (C) Principal component analysis of protein abundance from three populations.

way to differentiate the molecular effects in metal-rich oysters.

This study aimed to identify the signature biomarkers and investigate the responses under the complex metal contamination in the field. Therefore, the transcripts and the corresponding proteins identified with differential expression would provide more convincible results. In the present study, proteins were identified as positive correlations if they exhibited similar expression patterns between protein and transcript level (i.e., the transcript expressed higher, and the corresponding protein also expressed higher). Otherwise, they were named as the negative correlation. Compared to the Control, there were significant differences of 149 proteins in terms of their abundance, and 33 of them exhibited a positive and linear correlation again the transcriptional expression (R^2 = 0.8370, Fig. 4A and B). By contrast, more DEPs (230 proteins) were identified at High Zn–Cu–Ni–Cr (Station LFS) due to the much more critical levels of trace metals (Fig. S2B). Of these, 44 proteins exhibited similar expression patterns at the transcript level (DEGs), with linear correlation (R^2 = 0.7047, Fig. 4C and D). Interestingly, there was an intersection of those positively correlated proteins between these two stations (8 proteins). And 37 and 25 proteins were unique differentially expressed in oysters from High Zn–Cu–Ni–Cr (Station LFS) and High Cd (Station JZ), respectively (Fig. S2C). The significant linear correlation of the relative expression between RT-qPCR and the omic tools indicated the reliability of such unique tools in investigating the molecular dynamics (Fig. S3).

3.3. Similar alterations at two stations in PRE

Eight differentially expressed proteins were identified at both stations via iTRAQ and RNA-seq, with 4 up-regulation and 4 down-regulation (Fig. 5). A higher abundance of endoplasmic reticulum resident protein 29 (ERP29, 1.31-fold at Station LFS, 1.22-fold at Station JZ) was observed in oysters from both stations. ERP29 is a ubiquitous protein in the lumen of ER, participating in the protein-folding of normal cells and ER stress after stimulation (Mkrtchiana et al., 1998; Shnyder

and Hubbard, 2002). Therefore, the elevated Ag level might have resulted in endoplasmic reticulum (ER) stress in oyster *C. hongkongensis*. In the present study, a protein (ornithine aminotransferase, mitochondrial, OAT) located in the mitochondria matrix was observed with a higher abundance at both stations (1.33-fold at Station LFS, 1.52-fold at Station JZ). OAT is the enzyme catalyzing the synthesis of amino acids, which is associated with the normal function of mitochondria (Ginguay et al., 2017; Kobayashi et al., 1995). The role of OAT has been well-studied in plants, which is closely related to the tolerance to drought and salt (Anwar et al., 2018). Besides, the Golgi-associated plant pathogenesis-related protein 1 (GAPR-1) was significantly down-regulated in both stations (0.77-fold at Station LFS, 0.74-fold at Station JZ), indicating the potential impacts on the Golgi apparatus. It was also reported that GAPR-1 participated in the innate immune system, and the lower expression of GAPR-1 in the mussel was induced by the *Vibrio splendidus* infection (Eberle et al., 2002; Saco et al., 2020).

Interestingly, there were comparable Ag concentrations (around 23.7 µg/g) in oysters between Station JZ and Station LFS, which were also higher than Station QA (2.81 µg/g). Previous studies have investigated the effect of elevated Ag on living organisms, including mitochondria and ER (Loeffler and Lee, 1987; Xu et al., 2015; Yan et al., 2021; Yuan et al., 2017). Thus, the up-regulation of OAT might be the active compensation for the mitochondrial damage, indicating the potential toxicity of Ag in oysters. On the other hand, these 8 proteins could be the available biomarkers of higher metal contamination in oysters at both stations (Fig. 5). One explanation was that there was no dose-dependent effect on these proteins, although the concentrations of Zn, Cr, and Ni in three oyster populations were significantly different from each other and ranked as Control < High Cd < High Zn–Cu–Ni–Cr. Similar effects were observed in previous studies, such as zebrafish liver cell line under different levels of Cu exposure and oysters with high metal burdens across Southern China (Kwok et al., 2020; Li and Wang, 2021; Li et al., 2020).
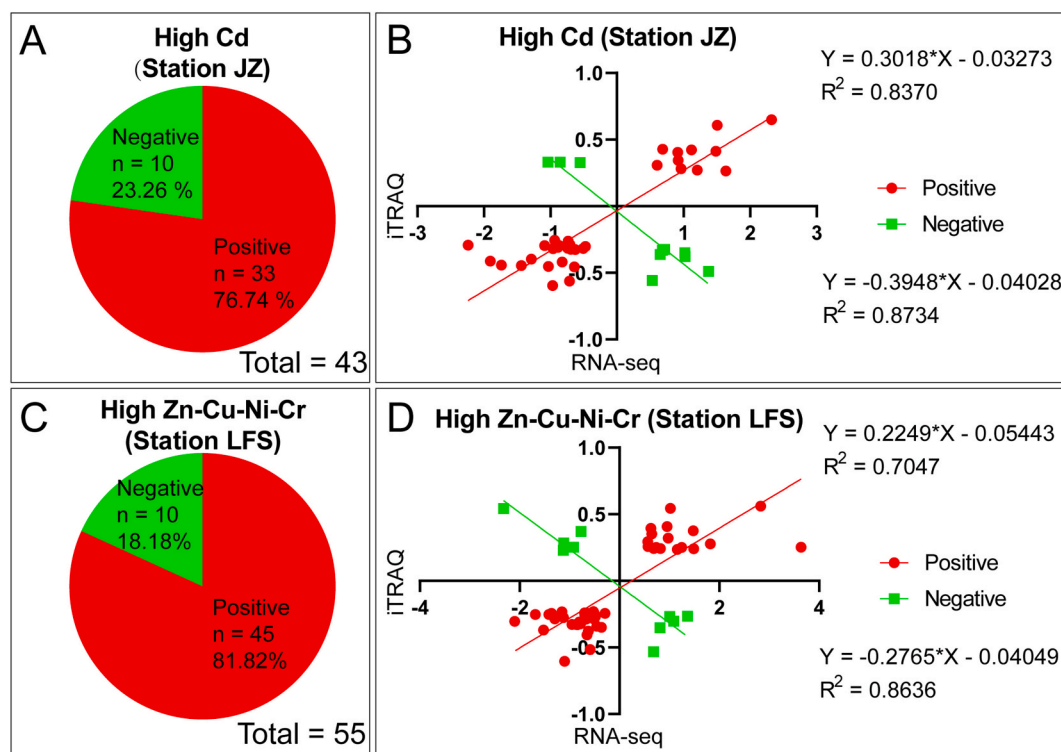

Fig. 4. Correlation between RNA-seq and iTRAQ. (A) and (B) High Cd (Station JZ). (C) and (D) High Zn–Cu–Ni–Cr (Station LFS). Only terms that were differentially expressed at both mRNA and protein levels were presented. The red color indicates the positive correlation, whereas the green color shows the negative. (For interpretation of the references to color in this figure legend, the reader is referred to the Web version of this article.)
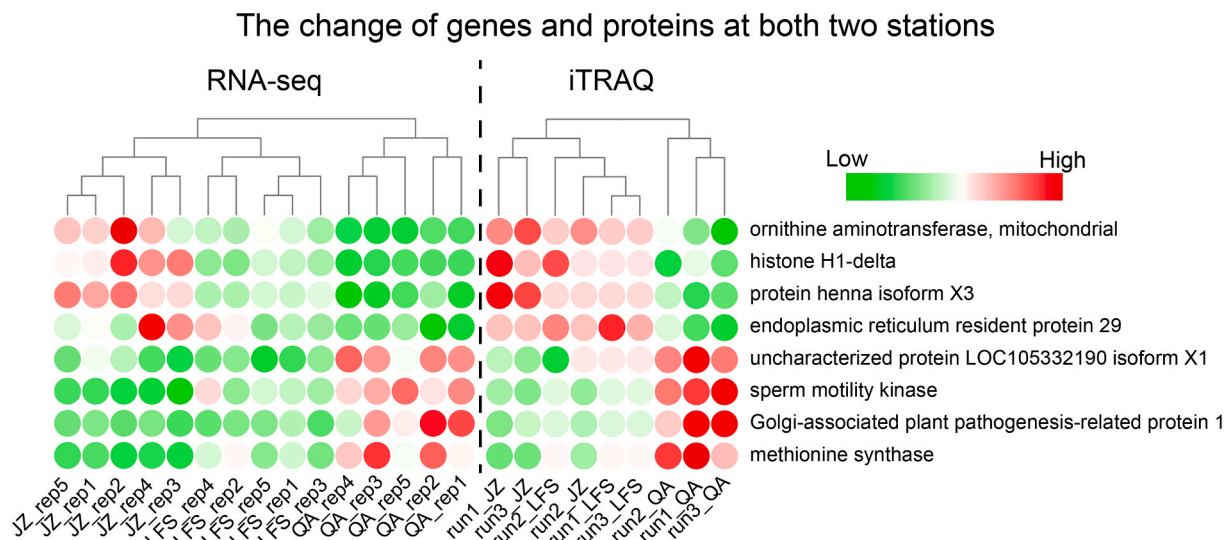
The change of genes and proteins at both two stations

Fig. 5. The expression level of proteins and genes that expressed differentially at both two stations. In the heatmap, red represents items with higher abundance and green for lower ones.

3.4. Genotoxicity in high Cd oysters

25 unique proteins only expressed differentially in the High Cd oysters (Fig. 6 and S2C), with 7 up-regulated and 18 down-regulated at both protein and transcript levels. Interestingly, 7 of 18 down-regulated proteins were involved in the genetic process (Fig. 6), including DNA replication and transcription.

The proliferation in the eukaryotic cell is highly controlled with the single run of DNA replication in each cell cycle. Specifically, a licensing system prevents the re-replication, a heterohexameric complex with six mini-chromosome maintenance proteins (MCM2-7) (Vijayraghavan and Schwacha, 2012). In the present study, 3 proteins annotated as MCM2, MCM5, and MCM7 were identified as the down-regulated proteins only in oysters from Station JZ (0.76–0.84-fold). Hence, a less abundance of the complex or some incomplete ones might result from their down-regulation, which would further cause the regulatory error. For example, DNA might be replicated more than once, or the replication might not be initiated normally. In mice, the low MCM expression would limit the origin licensing and replication stress (aberrant DNA replication patterns), further influencing hematopoietic stem cells (Alvarez et al., 2015).

Apart from the DNA replication, Cd may also pose damage to the transcription in oysters. A series of precise systems work to guarantee the storage and transfer of genetic information in organisms. In detail, 4 proteins in transcription with lower abundance at Station JZ were observed (Fig. 6): DNA-directed RNA polymerase II subunit RPB2 (RPB2, 0.82-fold), zinc finger CCCH domain-containing protein 18 (ZC3H18, 0.80-fold), splicing factor U2AF 50 kDa subunit (U2AF2, 0.80-fold), nucleolin-like (0.80-fold). As part of the core components in the transcriptional machinery between DNA-template and mRNA, RPB2 is responsible for synthesizing mRNA precursors (Acker et al., 1992). Nucleolin plays key roles in many pathways, including the maturation of pre-ribosomal RNA and initiation of RNA transcription (Mongelard and Bouvet, 2007). ZC3H18 could bind with core histone protein, directly associated with RNA production (Winczura et al., 2018). Furthermore, ZC3H18 could bind with the BRCA1 promoter and then induced homologous recombination (HR), implying its role in DNA repair (Kanakkanthara et al., 2019). The pre-mRNAs need splicing in the spliceosome before transported to the ribosome for translation.

In our study, the PCA of trace metals indicated that Cd might be the dominant metal contamination factor at High Cd (Station JZ), with concentrations up to 27.6 μg/g (the highest among three stations) in the gill filaments of oysters. In contrast to Station JZ, those changes in the genetic process were not observed at High Zn–Cu–Ni–Cr (Station LFS), although the oysters contained the highest Cu, Zn, Cr, and Ni. The genotoxicity of Cd in marine organisms has been well studied using the comet assay (Martins and Costa, 2014; Sarkar et al., 2015). Furthermore, Meng et al. (2017) demonstrated the decreased DNA repair ability might be the underlying mechanism of Cd in oyster *C. gigas* via indoor exposure at the protein levels. Therefore, the protein changes in the field-collected oysters with the highest Cd contents were consistent with the corresponding effect of Cd.

3.5. Critical threats on high Zn–Cu–Ni–Cr oysters

Station LFS contained typically higher contamination of four metals (Cu, Cr, Ni, and Zn) than the other two stations within the PRE; thus, it required further attention in this study (Fig. 1B). The integration between iTRAQ and RNA-seq identified 37 novel proteins that were only expressed differentially at High Zn–Cu–Ni–Cr and exhibited a similar pattern at both protein and transcript levels. Among these, 5 proteins in the cytoskeleton were detected with lower abundance. Both neurabin-1 (0.85-fold) and tight junction protein ZO-1 (TJP1,0.84-fold) bind to actin filaments, contributing to the formation of cytoskeleton and communication among cells (Fanning et al., 1998; Nakanishi et al., 1997). In addition, the doublecortin domain-containing protein 1 (DCDC1 or DCDC5) is involved in the cytokinesis via interacting with other cytoskeleton proteins, such as microtubule and dynein (Kaplan and Reiner, 2011). The lower abundances of two proteins were also found in the gill oysters from Station LFS: tektin-3 (TEKT3, 0.75-fold) and dynein beta chain (0.84-fold).

The cytoskeleton alteration has been documented in bivalves when they were under critical stress, including the elevated pH (Su et al., 2018), osmotic stress (Zhao et al., 2012), and hyperthermia (Truebano et al., 2010; Zhang et al., 2015). The cytoskeleton disruption was observed in oyster *C. hongkongensis* with extremely high Cu and Zn burdens (about 4000 and 40,000 μg/g, from Rongjiang Estuary) (Li and Wang, 2021; Li et al., 2020). In this study, the oysters at Station LFS accumulated up to 6000 μg/g Cu and around 20,000 μg/g Zn, and similar effects were observed there. In the eukaryotic cells, the cytoskeleton acts as the frame to maintain cell shape and contribute to cell mobility and signal transduction. The damaged cytoskeleton might directly lead to the abnormal functions of the cell. The outcome would be much more significant in oysters than other species (e.g., fish). Tektin
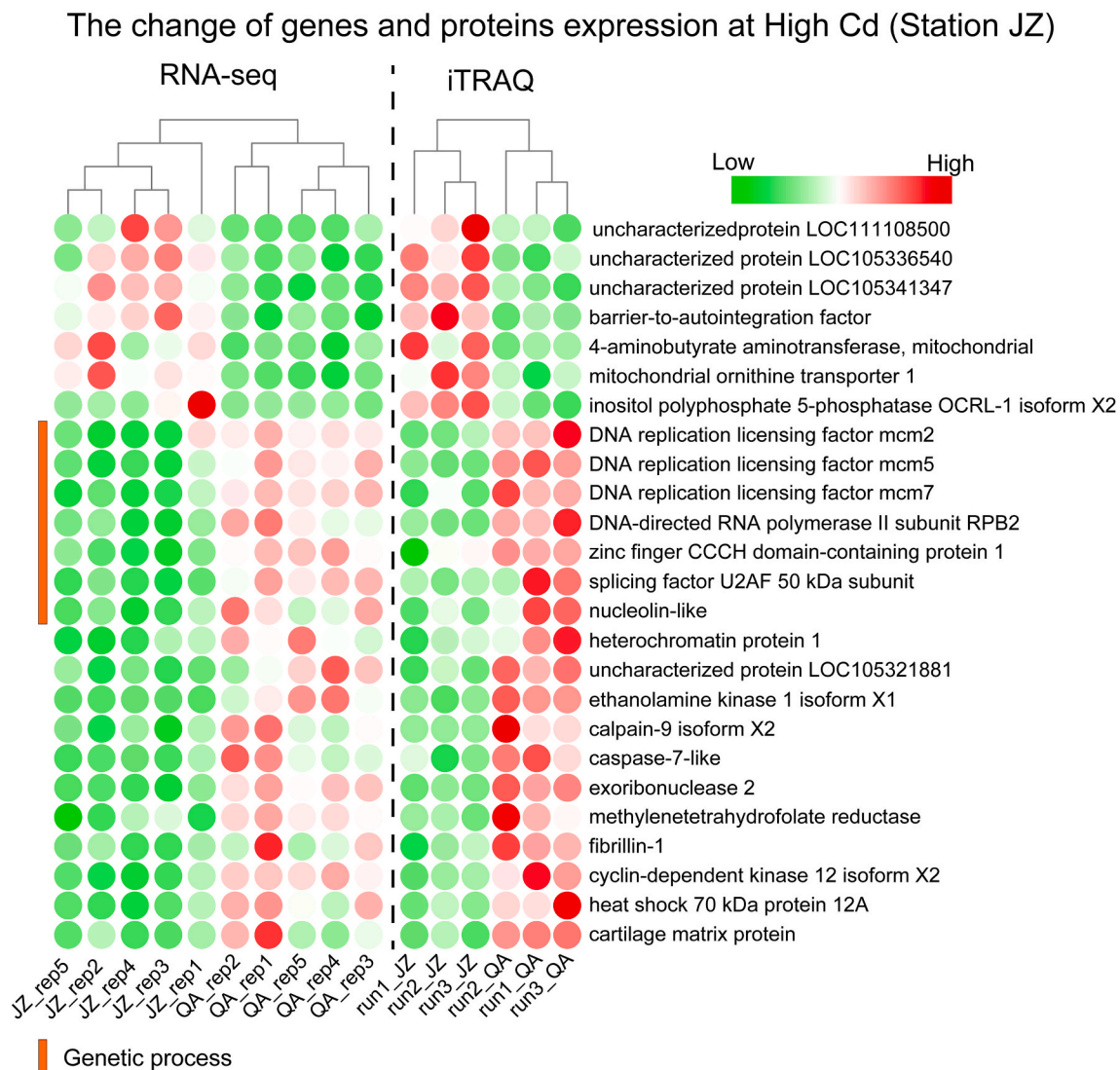
Fig. 6. The expression level of proteins and genes that only expressed differentially at High Cd (Station JZ), evaluated by RNA-seq and iTRAQ. The color bar at the bottom indicates the vital function them. In the heatmap, red represents items with higher abundance and green for the lower ones. (For interpretation of the references to color in this figure legend, the reader is referred to the Web version of this article.)

and dynein are indispensable elements in the cytoskeleton and play more significant roles in cilia and flagella for locomotion and sensory functions (Bastin and Schneider, 2019; Ibañez-Tallon et al., 2003). Apart from the above down-regulated proteins, the cilia- and flagella-associated protein 69 were expressed lower at High Zn–Cu–Ni–Cr (Station LFS) than Control (Station QA) with 0.77-fold. As mentioned before, the gill was the targeted tissue in detecting the molecular changes, implying the suppression of normal function in the gill. Gills are responsible for the gas exchange and food filtration of oysters. Therefore, the severe metal contaminations in PRE might influence the filtration of oyster *C. hongkongensis*, which is critical in acquiring nutrition from the ambient food particle environments.

Moreover, the elevated metal concentration in High Zn–Cu–Ni–Cr oysters (Station LFS) caused the chromosome damage, with 2 down-regulated proteins belonging to "Chromosome and associated proteins" (ko:03036). The centrosomal protein of 135 kDa (CEP135, 0.80-fold) is involved in regulating the centriole duplication and biosynthesis of centrosomes (Naveed et al., 2018). The knockdown of CEP135 by RNA interference would cause the dysfunction of microtubule and centrosomes in human cells (Hussain et al., 2012). The chromodomain-helicase-DNA-binding protein Mi-2 homolog (MI2B,

0.82-fold) could maintain the genome stability and remodel chromatin during the DNA-related process (Nagarajan et al., 2009).

3.6. Possible surviving mechanisms for high Zn–Cu–Ni–Cr oysters

One intriguing question is the tolerance of oysters from Station LFS when facing the typically higher levels of trace metals, especially for Cu and Zn. Apart from the 24 down-regulated proteins discussed before, 13 proteins were defined as up-regulated ones in oysters from the High Zn–Cu–Ni–Cr compared to the Control (Station QA). As shown in Fig. 7, 5 out of 13 up-regulated proteins belonged to aminoacyl-tRNA synthetases (i.e., asparagine, glycine, tyrosine, aspartate, and tryptophan), which catalyze the attachment of amino acids to tRNA (Alexander, 2013; Popow et al., 2012).

Before proteins functioning within the cell, they need to be translated from mRNA according to the correct interpretation (Rubio Gomez and Ibba, 2020). During the process, aminoacyl-tRNA synthetases are the most important ones, implementing the correct assembly between the amino acid and their codons (Kaiser et al., 2020). Only if there were enough tRNA, the translation process could go through smoothly. The higher abundance of 5 aminoacyl-tRNA synthetases might indicate more
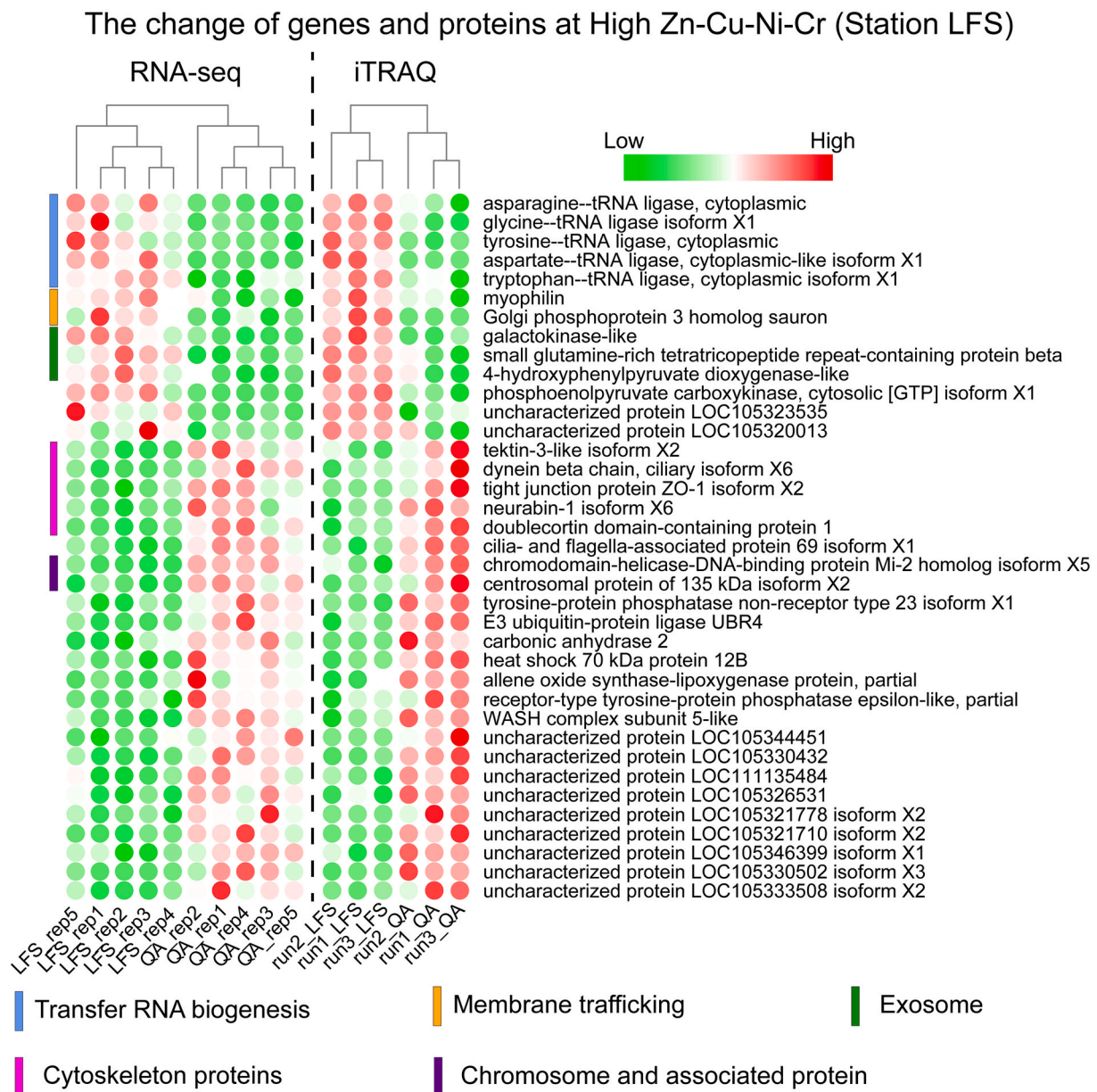
Fig. 7. The expression level of proteins and genes that only expressed differentially at High Zn–Cu–Ni–Cr (Station LFS), with results from RNA-seq and iTRAQ. The color bar in the bottom indicates the vital function group of them. In the heatmap, red represents items with higher abundance and green for lower one.

demands for translation, which might compensate for the damage of structural proteins from the hyperaccumulated metals in oysters. Furthermore, some studies reported that the increase of aminoacyl-tRNA synthetases contributed to positively coping with abiotic stress (El-Rami et al., 2018; Wei et al., 2014). For instance, the recruitment of some tRNA molecules is regarded as a strategy in yeasts to increase some required proteins under stress (Torrent et al., 2018).

Besides, 3 proteins in "Exosome" (ko: 04147) and 2 ones in "Membrane trafficking" (ko:04131) owned the higher abundances at Station LFS, including small glutamine-rich tetratricopeptide repeat-containing protein alpha (SGTA, 1.18-fold), galactokinase-like (GALK, 1.25-fold), 4-hydroxyphenylpyruvate dioxygenase (HPD, 1.18-fold), Golgi phosphoprotein 3 homolog Sauron (GOLPH3, 1.19-fold), and myophilin (1.19-fold) (Koh et al., 2016; Roberts et al., 2015; Sechi et al., 2014). Exosome is a type of extracellular vesicle in most eukaryotic cells, which participates in signal transduction by transporting small molecules (e.g., mRNA, proteins) (Jones et al., 2018). Besides, the exosome works as a cleaner to excrete the damaged proteins, thus maintaining cellular

homeostasis (Desdín-Micó and Mittelbrunn, 2017). The cytoskeleton might be disrupted by the high metal burdens at Station LFS, implying the potential impairment of signal transduction relied on it. Furthermore, the excess metal ions would attack the proteins directly or via inducing reactive oxidative species indirectly (Li and Wang, 2021). GOLPH3 has been identified with protein trafficking, receptor recycling, and further related to cell transformation (Scott and Chin, 2010). In summary, the activated exosome and membrane part in High Zn–Cu–Ni–Cr oysters (Station LFS) could help the oyster perform normal signal transduction and maintain cellular homeostasis when the high levels of metals might injure the cytoskeleton and some proteins.

4. Conclusion

For the first time, this study adopted the integrated analysis of RNA-seq and iTRAQ to investigate the ecotoxicological effects of trace metals on oyster *C. hongkongensis* (a bioindicator for metal contamination levels). The metal concentrations in oysters were different among the

three oyster populations, indicating the spatial distribution of metal contamination in the PRE. A similar pattern (visualized by PCA) was observed between the metal accumulations in oysters and their protein profiles (Figs. 2 and 3C). Oysters from Station QA accumulated the lowest levels of all six trace metals and were labeled as 'Control' in the bioinformatics analysis. A total of 70 proteins were expressed differentially in oysters under metal stress, and those proteins exhibited similar alteration patterns at both protein and RNA levels. Among these proteins, 8 proteins at both stations could be the potential biomarkers for Ag level, such as the components in mitochondria (OAT) and endoplasmic reticulum (ERP29). There were 25 unique proteins at High Cd (Station JZ), and 7 of them were related to genetic materials (DNA and RNA) , including MCM subunits and RPB2. These differential expressions implied the potential genetic toxicity from Cd and could be the potential markers for Cd pollution. The remaining 37 proteins were solely observed in High Zn–Cu–Ni–Cr oysters, which could be used to indicate the relative levels of Cu, Zn, Cr, and Ni, such as TEKT3 and CEP135. The hyperaccumulated metals, especially for Cu, and Zn, would cause the disruption of structural proteins (i.e., cytoskeleton and chromosome). Nonetheless, the higher abundances of proteins related to tRNA generation and exosome would help oysters to cope with the severe stress from metals. Altogether, our study provided the molecular alteration on oysters stressed by metals in the PRE and further proposed some potential biomarkers which could be used in ecological assessments. However, we only discussed the limited contribution of trace metals to expressional profiles in oysters but overlooked other factors.. Therefore, it will be important to further test the applicability of these molecular biomarkers in larger environmental settings.

Declaration of competing interest

The authors declare that they have no known competing financial interests or personal relationships that could have appeared to influence the work reported in this paper.

Acknowledgement

Appendix A. Supplementary data

Supplementary data to this article can be found online at https://doi.org/10.1016/j.envpol.2021.117533.

Author contribution statement

Yunlong Li:Conceptualization, Investigation, Writing. Wen-Xiong Wang: Conceptualization, Writing

References

Acker, J., Wintzerith, M., Vigneron, M., Kédinger, C., 1992. Primary structure of the second largest subunit of human RNA polymerase II (or B). J. Mol. Biol. 226, 1295–1299.

Alexander, R.W., 2013. tRNA synthetases. In: Lennarz, W.J., Lane, M.D. (Eds.), Encyclopedia of Biological Chemistry, second ed. Academic Press, Waltham, pp. 441–444.

Alvarez, S., Díaz, M., Flach, J., Rodriguez-Acebes, S., López-Contreras, A.J., Martínez, D., Cañamero, M., Fernández-Capetillo, O., Isern, J., Passegué, E., Méndez, J., 2015. Replication stress caused by low MCM expression limits fetal erythropoiesis and hematopoietic stem cell functionality. Nat. Commun. 6, 8548.

Anwar, A., She, M., Wang, K., Riaz, B., Ye, X., 2018. Biological roles of ornithine aminotransferase (OAT) in plant stress tolerance: present progress and future perspectives. Int. J. Mol. Sci. 19, 3681.

Bastin, B.R., Schneider, S.Q., 2019. Taxon-specific expansion and loss of tektins inform metazoan ciliary diversity. BMC Evol. Biol. 19, 40.

Bjärnmark, N.A., Yarra, T., Churcher, A.M., Felix, R.C., Clark, M.S., Power, D.M., 2016. Transcriptomics provides insight into Mytilus galloprovincialis (Mollusca: Bivalvia) mantle function and its role in biomineralisation. Mar. Genomics 27, 37–45.

Blencowe, B.J., 2006. Alternative splicing: new insights from global analyses. Cell 126, 37–47.

Bolger, A.M., Lohse, M., Usadel, B., 2014. Trimmomatic: a flexible trimmer for Illumina sequence data. Bioinformatics 30, 2114–2120.

Camacho, C., Coulouris, G., Avagyan, V., Ma, N., Papadopoulos, J., Bealer, K., Madden, T.L., 2009. BLAST+: architecture and applications. BMC Bioinf. 10, 421.

Carneiro, R.L., Requião, R.D., Rossetto, S., Domitrovic, T., Palhano, F.L., 2019. Codon stabilization coefficient as a metric to gain insights into mRNA stability and codon bias and their relationships with translation. Nucleic Acids Res. 47, 2216–2228.

Chan, C.Y., Wang, W.-X., 2019. Biomarker responses in oysters Crassostrea hongkongensis in relation to metal contamination patterns in the Pearl River Estuary, Southern China. Environ. Pollut. 251, 264–276.

Desdín-Micó, G., Mittelbrunn, M., 2017. Role of exosomes in the protection of cellular homeostasis. Cell Adhes. Migrat. 11, 127–134.

Deutsch, E.W., Mendoza, L., Shteynberg, D., Farrah, T., Lam, H., Tasman, N., Sun, Z., Nilsson, E., Pratt, B., Prazen, B., Eng, J.K., Martin, D.B., Nesvizhskii, A.I., Aebersold, R., 2010. A guided tour of the trans-proteomic pipeline. Proteomics 10, 1150–1159.

Dineshram, R., Q, Q., Sharma, R., Chandramouli, K., Yalamanchili, H.K., Chu, I., Thiyagarajan, V., 2015. Comparative and quantitative proteomics reveal the adaptive strategies of oyster larvae to ocean acidification. Proteomics 15, 4120–4134.

Dong, L., Su, J., Ah Wong, L., Cao, Z., Chen, J.-C., 2004. Seasonal variation and dynamics of the Pearl River plume. Continent. Shelf Res. 24, 1761–1777.

Eberle, H.B., Serrano, R.L., Füllekrug, J., Schlosser, A., Lehmann, W.D., Lottspeich, F., Kaloyanova, D., Wieland, F.T., Helms, J.B., 2002. Identification and characterization of a novel human plant pathogenesis-related protein that localizes to lipid-enriched microdomains in the Golgi complex. J. Cell Sci. 115, 827.

El-Rami, F., Kong, X., Parikh, H., Zhu, B., Stone, V., Kitten, T., Xu, P., 2018. Analysis of essential gene dynamics under antibiotic stress in Streptococcus sanguinis. Microbiology 164, 173–185.

Eng, J.K., Jahan, T.A., Hoopmann, M.R., 2013. Comet: an open-source MS/MS sequence database search tool. Proteomics 13, 22–24.

Fanning, A.S., Jameson, B.J., Jesaitis, L.A., Anderson, J.M., 1998. The tight junction protein ZO-1 establishes a link between the transmembrane protein occludin and the actin cytoskeleton. J. Biol. Chem. 273, 29745–29753.

Ginguay, A., Cynober, L., Curis, E., Nicolis, I., 2017. Ornithine aminotransferase, an important glutamate-metabolizing enzyme at the crossroads of multiple metabolic pathways. Biology 6, 18.

Guerette, P.A., Hoon, S., Seow, Y., Raida, M., Masic, A., Wong, F.T., Ho, V.H.B., Kong, K. W., Demirel, M.C., Pena-Francesch, A., Amini, S., Tay, G.Z., Ding, D., Miserez, A., 2013. Accelerating the design of biomimetic materials by integrating RNA-seq with proteomics and materials science. Nat. Biotechnol. 31, 908–915.

Haider, S., Pal, R., 2013. Integrated analysis of transcriptomic and proteomic data. Curr. Genom. 14, 91–110.

Higdon, R., Kala, J., Wilkins, D., Yan, J.F., Sethi, M.K., Lin, L., Liu, S., Montague, E., Janko, I., Choiniere, J., Kolker, N., Hancock, W.S., Kolker, E., Fanayan, S., 2017. Integrated proteomic and transcriptomic-based approaches to identifying signature biomarkers and pathways for elucidation of daoy and UW228 subtypes. Proteomes 5, 5.

HKEPD, 2020. Marine Water Quality in Hong Kong in 2019.

HKTDC, 2020. PRD Economic Profile.

Hussain, Muhammad S., Baig, Shahid M., Neumann, S., Nürnberg, G., Farooq, M., Ahmad, I., Alef, T., Hennies, Hans C., Technau, M., Altmüller, J., Frommolt, P., Thiele, H., Noegel, Angelika A., Nürnberg, P., 2012. A truncating mutation of CEP135 causes primary microcephaly and disturbed centrosomal function. Am. J. Hum. Genet. 90, 871–878.

Ibañez-Tallon, I., Heintz, N., Omran, H., 2003. To beat or not to beat: roles of cilia in development and disease. Hum. Mol. Genet. 12, R27–R35.

Jones, L.B., Bell, C.R., Bibb, K.E., Gu, L., Coats, M.T., Matthews, Q.L., 2018. Pathogens and their effect on exosome biogenesis and composition. Biomedicines 6, 79.

Kaiser, F., Krautwurst, S., Salentin, S., Haupt, V.J., Leberecht, C., Bittrich, S., Labudde, D., Schroeder, M., 2020. The structural basis of the genetic code: amino acid recognition by aminoacyl-tRNA synthetases. Sci. Rep. 10, 12647.

Kammers, K., Cole, R.N., Tiengwe, C., Ruczinski, I., 2015. Detecting significant changes in protein abundance. EuPA Open Proteomics 7, 11–19.

Kanakkanthara, A., Huntoon, C.J., Hou, X., Zhang, M., Heinzen, E.P., O'Brien, D.R., Oberg, A.L., John Weroha, S., Kaufmann, S.H., Karnitz, L.M., 2019. ZC3H18 specifically binds and activates the BRCA1 promoter to facilitate homologous recombination in ovarian cancer. Nat. Commun. 10, 4632.

Kanehisa, M., Sato, Y., Morishima, K., 2016. BlastKOALA and GhostKOALA: KEGG tools for functional characterization of genome and metagenome sequences. J. Mol. Biol. 428, 726–731.

Kaplan, A., Reiner, O., 2011. Linking cytoplasmic dynein and transport of Rab8 vesicles to the midbody during cytokinesis by the doublecortin domain-containing 5 protein. J. Cell Sci. 124, 3989.

Kaur, P., Rizk, N.M., Ibrahim, S., Younes, N., Uppal, A., Dennis, K., Karve, T., Blakeslee, K., Kwagyan, J., Zirie, M., Ressom, H.W., Cheema, A.K., 2012. iTRAQ-based quantitative protein expression profiling and MRM verification of markers in Type 2 diabetes. J. Proteome Res. 11, 5527–5539.

Ke, C., Wang, W.-X., 2001. Bioaccumulation of Cd, Se, and Zn in an estuarine oyster (Crassostrea rivularis) and a coastal oyster (Saccostrea glomerata). Aquat. Toxicol. 56, 33–51.

Kessner, D., Chambers, M., Burke, R., Agus, D., Mallick, P., 2008. ProteoWizard: open source software for rapid proteomics tools development. Bioinformatics 24, 2534–2536.

Kobayashi, T., Ogawa, H., Kasahara, M., Shiozawa, Z., Matsuzawa, T., 1995. A single amino acid substitution within the mature sequence of ornithine aminotransferase obstructs mitochondrial entry of the precursor. Am. J. Hum. Genet. 57, 284–291.

Koh, Y.Q., Peiris, H.N., Vaswani, K., Reed, S., Rice, G.E., Salomon, C., Mitchell, M.D., 2016. Characterization of exosomal release in bovine endometrial intercaruncular stromal cells. Reprod. Biol. Endocrinol. 14, 78-78.

Kumar, D., Bansal, G., Narang, A., Basak, T., Abbas, T., Dash, D., 2016. Integrating transcriptome and proteome profiling: strategies and applications. Proteomics 16, 2533–2544.

Kwok, M.L., Hu, X.L., Meng, Q., Chan, K.M., 2020. Whole-transcriptome sequencing (RNA-seq) analyses of the zebrafish liver cell line, ZFL, after acute exposure to Cu2+ ions. Metall 12, 732–751.

Lam, K., Morton, B., 2003. Mitochondrial DNA and morphological identification of a new species of Crassostrea (Bivalvia: ostreidae) cultured for centuries in the Pearl River Delta, Hong Kong, China. Aquaculture 228, 1–13.

Langmead, B., Salzberg, S.L., 2012. Fast gapped-read alignment with Bowtie 2. Nat. Methods 9, 357.

Li, B., Dewey, C.N., 2011. RSEM: accurate transcript quantification from RNA-Seq data with or without a reference genome. BMC Bioinf. 12, 323.

Li, L., Wu, X., Yu, Z., 2013. Genetic diversity and substantial population differentiation in Crassostrea hongkongensis revealed by mitochondrial DNA. Mar. Genomics 11, 31–37.

Li, Y., Tsim, K.W.-K., Wang, W.-X., 2021. Copper promoting oyster larval growth and settlement: molecular insights from RNA-seq. Sci. Total Environ. 784, 147159.

Li, Y., Wang, W.-X., 2021. Protein molecular responses of field-collected oysters Crassostrea hongkongensis with greatly varying Cu and Zn body burdens. Aquat. Toxicol. 232, 105749.

Li, Y., Wang, Z., Zhao, Z., Cui, Y., 2019. iTRAQ-based proteome profiling of hyposaline responses in zygotes of the Pacific oyster Crassostrea gigas. Comp. Biochem. Physiol. Genom. Proteomics 30, 14–24.

Li, Y., Zhang, X., Meng, J., Chen, J., You, X., Shi, Q., Wang, W.-X., 2020. Molecular responses of an estuarine oyster to multiple metal contamination in Southern China revealed by RNA-seq. Sci. Total Environ. 701, 134648.

Liu, X., Li, D., Song, G., 2017. Assessment of heavy metal levels in surface sediments of estuaries and adjacent coastal areas in China. Front. Earth Sci. 11, 85–94.

Liu, X., Wang, W.-X., 2016a. Antioxidant and detoxification responses of oysters Crassostrea hongkongensis in a multimetal-contaminated estuary. Environ. Toxicol. Chem. 35, 2798–2805.

Liu, X., Wang, W.-X., 2016b. Physiological and cellular responses of oysters (Crassostrea hongkongensis) in a multimetal-contaminated estuary. Environ. Toxicol. Chem. 35, 2577–2586.

Loeffler, K.U., Lee, W.R., 1987. Argyrosis of the lacrimal sac. Graefes Arch. Clin. Exp. Ophthalmol. 225, 146–150.

Love, M.I., Huber, W., Anders, S., 2014. Moderated estimation of fold change and dispersion for RNA-seq data with DESeq2. Genome Biol. 15, 550.

Lu, G., Pan, K., Zhu, A., Dong, Y., Wang, W.-X., 2020. Spatial-temporal variations and trends predication of trace metals in oysters from the Pearl River Estuary of China during 2011–2018. Environ. Pollut. 264, 114812.

Lu, G., Zhu, A., Fang, H., Dong, Y., Wang, W.-X., 2019. Establishing baseline trace metals in marine bivalves in China and worldwide: meta-analysis and modeling approach. Sci. Total Environ. 669, 746–753.

Luo, L., Ke, C., Guo, X., Shi, B., Huang, M., 2014. Metal accumulation and differentially expressed proteins in gill of oyster (Crassostrea hongkongensis) exposed to long-term heavy metal-contaminated estuary. Fish Shellfish Immunol. 38, 318–329.

Martins, M., Costa, P.M., 2014. The comet assay in environmental risk assessment of marine pollutants: applications, assets and handicaps of surveying genotoxicity in non-model organisms. Mutagenesis 30, 89–106.

Meng, J., Wang, W.-X., Li, L., Zhang, G., 2018. Tissue-specific molecular and cellular toxicity of Pb in the oyster (Crassostrea gigas): mRNA expression and physiological studies. Aquat. Toxicol. 198, 257–268.

Meng, J., Wang, W., Li, L., Yin, Q., Zhang, G., 2017. Cadmium effects on DNA and protein metabolism in oyster (Crassostrea gigas) revealed by proteomic analyses. Sci. Rep. 7, 11716.

Mkrtchiana, S., Baryshev, M., Matvijenko, O., Sharipo, A., Sandalova, T., Schneider, G., Ingelman-Sundberg, M., 1998. Oligomerization properties of ERp29, an endoplasmic reticulum stress protein. FEBS Lett. 431, 322–326.

Mongelard, F., Bouvet, P., 2007. Nucleolin: a multiFACeTed protein. Trends Cell Biol. 17, 80–86.

Moritz, C.P., Mühlhaus, T., Tenzer, S., Schulenborg, T., Friauf, E., 2019. Poor transcript-protein correlation in the brain: negatively correlating gene products reveal neuronal polarity as a potential cause. J. Neurochem. 149, 582–604.

Nagarajan, P., Onami, T.M., Rajagopalan, S., Kania, S., Donnell, R., Venkatachalam, S., 2009. Role of chromodomain helicase DNA-binding protein 2 in DNA damage response signaling and tumorigenesis. Oncogene 28, 1053–1062.

Nakanishi, H., Obaishi, H., Satoh, A., Wada, M., Mandai, K., Satoh, K., Nishioka, H., Matsuura, Y., Mizoguchi, A., Takai, Y., 1997. Neurabin: a novel neural tissue-specific actin filament-binding protein involved in neurite formation. J. Cell Biol. 139, 951–961.

Naveed, M., Kazmi, S.K., Amin, M., Asif, Z., Islam, U., Shahid, K., Tehreem, S., 2018. Comprehensive review on the molecular genetics of autosomal recessive primary microcephaly (MCPH). Genet. Res. 100, e7.

Nesvizhskii, A.I., Keller, A., Kolker, E., Aebersold, R., 2003. A statistical model for identifying proteins by tandem mass spectrometry. Anal. Chem. 75, 4646–4658.

Niu, A., Ma, J., Gao, Y., Xu, S., Lin, C., 2020. Mangrove soil-borne trace elements in Qi'ao island: implications for understanding terrestrial input of trace elements into part of the Pearl River Estuary. Appl. Sci. 10.

O'Brien, J., Hayder, H., Zayed, Y., Peng, C., 2018. Overview of microRNA biogenesis, mechanisms of actions, and circulation. Front. Endocrinol. 9, 402.

Pan, K., Wang, W.-X., 2009. Biodynamics to explain the difference of copper body concentrations in five marine bivalve species. Environ. Sci. Technol. 43, 2137–2143.

Parkes, G.M., Niranjan, M., 2019. Uncovering extensive post-translation regulation during human cell cycle progression by integrative multi-omics analysis. BMC Bioinf. 20, 536.

Peng, Z., He, S., Gong, W., Xu, F., Pan, Z., Jia, Y., Geng, X., Du, X., 2018. Integration of proteomic and transcriptomic profiles reveals multiple levels of genetic regulation of salt tolerance in cotton. BMC Plant Biol. 18, 128.

Pintado-Herrera, M.G., Wang, C., Lu, J., Chang, Y.-P., Chen, W., Li, X., Lara-Martín, P.A., 2017. Distribution, mass inventories, and ecological risk assessment of legacy and emerging contaminants in sediments from the Pearl River Estuary in China. J. Hazard Mater. 323, 128–138.

Popow, J., Schleiffer, A., Martinez, J., 2012. Diversity and roles of (t)RNA ligases. Cell. Mol. Life Sci. 69, 2657–2670.

Roberts, J.D., Thapaliya, A., Martínez-Lumbreras, S., Krysztofinska, E.M., Isaacson, R.L., 2015. Structural and functional insights into small, glutamine-rich, tetratricopeptide repeat protein alpha. Front. Mol. Biosci. 2.

Rubio Gomez, M.A., Ibba, M., 2020. Aminoacyl-tRNA Synthetases. RNA.

Saco, A., Rey-Campos, M., Novoa, B., Figueras, A., 2020. Transcriptomic response of mussel gills after a vibrio splendidus infection demonstrates their role in the immune response. Front. Immunol. 11.

Sarkar, A., Bhagat, J., Ingole, B.S., Rao, D.P., Markad, V.L., 2015. Genotoxicity of cadmium chloride in the marine gastropod Nerita chamaeleon using comet assay and alkaline unwinding assay. Environ. Toxicol. 30, 177–187.

Scott, K.L., Chin, L., 2010. Signaling from the Golgi: mechanisms and models for Golgi phosphoprotein 3–mediated oncogenesis. Clin. Canc. Res. 16, 2229.

Sechi, S., Colotti, G., Belloni, G., Mattei, V., Frappaolo, A., Raffa, G.D., Fuller, M.T., Giansanti, M.G., 2014. GOLPH3 is essential for contractile ring formation and Rab11 localization to the cleavage site during cytokinesis in Drosophila melanogaster. PLoS Genet. 10 e1004305-e1004305.

Shnyder, S.D., Hubbard, M.J., 2002. ERp29 is a ubiquitous resident of the endoplasmic reticulum with a distinct role in secretory protein production. J. Histochem. Cytochem. 50, 557–566.

Shteynberg, D., Deutsch, E.W., Lam, H., Eng, J.K., Sun, Z., Tasman, N., Mendoza, L., Moritz, R.L., Aebersold, R., Nesvizhskii, A.I., 2011. iProphet: multi-level integrative analysis of shotgun proteomic data improves peptide and protein identification rates and error estimates. Mol. Cell. Proteomics 10. M111.007690.

Su, W., Rong, J., Zha, S., Yan, M., Fang, J., Liu, G., 2018. Ocean acidification affects the cytoskeleton, lysozymes, and nitric oxide of hemocytes: a possible explanation for the hampered phagocytosis in blood clams, Tegillarca granosa. Front. Physiol. 9.

Tan, Q.-G., Zhou, W., Wang, W.-X., 2018. Modeling the toxicokinetics of multiple metals in the oyster Crassostrea hongkongensis in a dynamic estuarine environment. Environ. Sci. Technol. 52, 484–492.

Tang, D., Liu, X., He, H., Cui, Z., Gan, H., Xia, Z., 2020. Distribution, sources and ecological risks of organochlorine compounds (DDTs, HCHs and PCBs) in surface sediments from the Pearl River Estuary, China. Mar. Pollut. Bull. 152, 110942.

Tang, L., Sheng, J., Ji, X., Cao, W., Liu, D., 2009. Investigation of three-dimensional circulation and hydrography over the Pearl River Estuary of China using a nested-grid coastal circulation model. Ocean Dynam. 59, 899.

Taylor, R.C., Webb Robertson, B.-J.M., Markillie, L.M., Serres, M.H., Linggi, B.E., Aldrich, J.T., Hill, E.A., Romine, M.F., Lipton, M.S., Wiley, H.S., 2013. Changes in translational efficiency is a dominant regulatory mechanism in the environmental response of bacteria. Integr. Biol. 5, 1393–1406.

Torrent, M., Chalancon, G., de Groot, N.S., Wuster, A., Madan Babu, M., 2018. Cells alter their tRNA abundance to selectively regulate protein synthesis during stress conditions. Sci. Signal. 11, eaat6409.

Truebano, M., Burns, G., Thorne, M.A.S., Hillyard, G., Peck, L.S., Skibinski, D.O.F., Clark, M.S., 2010. Transcriptional response to heat stress in the Antarctic bivalve Laternula elliptica. J. Exp. Mar. Biol. Ecol. 391, 65–72.

Vailati-Riboni, M., Palombo, V., Loor, J.J., 2017. What are omics sciences? In: Ametaj, B. N. (Ed.), Periparturient Diseases of Dairy Cows: A Systems Biology Approach. Springer International Publishing, Cham, pp. 1–7.

Vijayraghavan, S., Schwacha, A., 2012. The eukaryotic Mcm2-7 replicative helicase. In: MacNeill, S. (Ed.), The Eukaryotic Replisome: a Guide to Protein Structure and Function. Springer Netherlands, Dordrecht, pp. 113–134.

Wang, H., Guo, X., 2008. Identification of Crassostrea ariakensis and related oysters by multiplex species-specific PCR. J. Shellfish Res. 27, 481–487.

Wang, W.-X., Rainbow, P.S., 2020. Pollution in the Pearl River estuary. In: Wang, W.-X., Rainbow, P.S. (Eds.), Environmental Pollution of the Pearl River Estuary, China: Status and Impact of Contaminants in a Rapidly Developing Region. Springer Berlin Heidelberg, Berlin, Heidelberg, pp. 13–35.

Wang, W.-X., Yang, Y., Guo, X., He, M., Guo, F., Ke, C., 2011. Copper and zinc contamination in oysters: subcellular distribution and detoxification. Environ. Toxicol. Chem. 30, 1767–1774.

Wei, N., Shi, Y., Truong, Lan N., Fisch, Kathleen M., Xu, T., Gardiner, E., Fu, G., Hsu, Y.-Shiuan O., Kishi, S., Su, Andrew I., Wu, X., Yang, X.-L., 2014. Oxidative stress diverts tRNA synthetase to nucleus for protection against DNA damage. Mol. Cell. 56, 323–332.

Weng, N., Wang, W.-X., 2015. Reproductive responses and detoxification of estuarine oyster Crassostrea hongkongensis under Metal Stress: a Seasonal Study. Environ. Sci. Technol. 49, 3119–3127.

Wiese, S., Reidegeld, K.A., Meyer, H.E., Warscheid, B., 2007. Protein labeling by iTRAQ: a new tool for quantitative mass spectrometry in proteome research. Proteomics 7, 340–350.

Winczura, K., Schmid, M., Iasillo, C., Molloy, K.R., Harder, L.M., Andersen, J.S., LaCava, J., Jensen, T.H., 2018. Characterizing ZC3H18, a multi-domain protein at the Interface of RNA production and destruction decisions. Cell Rep. 22, 44–58.

Xiao, R., Bai, J., Wang, J., Lu, Q., Zhao, Q., Cui, B., Liu, X., 2014. Polycyclic aromatic hydrocarbons (PAHs) in wetland soils under different land uses in a coastal estuary: toxic levels, sources and relationships with soil organic matter and water-stable aggregates. Chemosphere 110, 8–16.

Xu, L., Shi, C., Shao, A., Li, X., Cheng, X., Ding, R., Wu, G., Chou, L.L., 2015. Toxic responses in rat embryonic cells to silver nanoparticles and released silver ions as analyzed via gene expression profiles and transmission electron microscopy. Nanotoxicology 9, 513–522.

Yan, L.-R., Wang, D.-X., Liu, H., Zhang, X.-X., Zhao, H., Hua, L., Xu, P., Li, Y.-S., 2014. A pro-atherogenic HDL profile in coronary heart disease patients: an iTRAQ labelling-based proteomic approach. PloS One 9, e98368.

Yan, N., Tang, B.Z., Wang, W.-X., 2021. Intracellular trafficking of silver nanoparticles and silver ions determined their specific mitotoxicity to the zebrafish cell line. Environ. Sci.: Nano 8, 1364–1375.

Yin, Q., Wang, W.-X., 2017. Relating metals with major cations in oyster Crassostrea hongkongensis: a novel approach to calibrate metals against salinity. Sci. Total Environ. 577, 299–307.

Yu, H., Liu, Y., Han, C., Fang, H., Weng, J., Shu, X., Pan, Y., Ma, L., 2021. Polycyclic aromatic hydrocarbons in surface waters from the seven main river basins of China: spatial distribution, source apportionment, and potential risk assessment. Sci. Total Environ. 752, 141764.

Yu, X.-J., Pan, K., Liu, F., Yan, Y., Wang, W.-X., 2013. Spatial variation and subcellular binding of metals in oysters from a large estuary in China. Mar. Pollut. Bull. 70, 274–280.

Yuan, K., Qing, Q., Wang, Y., Lin, F., Chen, B., Luan, T., Wang, X., 2020. Characteristics of chlorinated and brominated polycyclic aromatic hydrocarbons in the Pearl River Estuary. Sci. Total Environ. 739, 139774.

Yuan, L., Gao, T., He, H., Jiang, F.L., Liu, Y., 2017. Silver ion-induced mitochondrial dysfunction via a nonspecific pathway. Toxicol. Res. 6, 621–630.

Zhang, L., Gurskaya, N.G., Merzlyak, E.M., Staroverov, D.B., Mudrik, N.N., Samarkina, O. N., Vinokurov, L.M., Lukyanov, S., Lukyanov, K.A., 2007. Method for real-time monitoring of protein degradation at the single cell level. Biotechniques 42, 446–450.

Zhang, Y., Mao, F., Xiao, S., Yu, H., Xiang, Z., Xu, F., Li, J., Wang, L., Xiong, Y., Chen, M., Bao, Y., Deng, Y., Huo, Q., Zhang, L., Liu, W., Li, X., Ma, H., Zhang, Y., Mu, X., Liu, M., Zheng, H., Wong, N.-K., Yu, Z., 2021. Comparative genomics reveals evolutionary drivers of sessile life and left-right shell asymmetry in bivalves. bioRxiv, 2021.2003 2018, 435778.

Zhang, Y., Sun, J., Mu, H., Li, J., Zhang, Y., Xu, F., Xiang, Z., Qian, P.-Y., Qiu, J.-W., Yu, Z., 2015. Proteomic basis of stress responses in the gills of the Pacific oyster Crassostrea gigas. J. Proteome Res. 14, 304–317.

Zhao, X., Qiu, W., Zheng, Y., Xiong, J., Gao, C., Hu, S., 2019. Occurrence, distribution, bioaccumulation, and ecological risk of bisphenol analogues, parabens and their metabolites in the Pearl River Estuary, South China. Ecotoxicol. Environ. Saf. 180, 43–52.

Zhao, X., Yu, H., Kong, L., Li, Q., 2012. Transcriptomic responses to salinity stress in the Pacific oyster Crassostrea gigas. PloS One 7, e46244.